SUBMITTED TO THE 1964 DUBNA INTERNATIONAL CONFERENCE ON HIGH ENERGY PHYSICS

CERN/TC/PHYSICS 64-32
29.7.1964

RESONANCE PRODUCTION IN 4-PRONG INTERACTIONS OF 8 GeV/c π^+ IN HYDROGEN

AACHEN - BERLIN - CERN COLLABORATION

M. Deutschmann, R. Krichel, R. Speth, H. Weber and W. Woischnig,
I. Physikalisches Institut der Technischen Hochschule, Aachen

C. Grote, J. Klugow, A. Meyer and S. Nowak,
Forschungsstelle fur Physik hoher Energien der Deutschen Akademie der Wissenschaften zu Berlin - Zeuthen

S. Brandt, V.T. Cocconi, O. Czyzewski+, J. Danysz+, P. Dalpiaz*, G. Kellner** and D.R.O. Morrison,
CERN - European Organization for Nuclear Research, Geneva

There has been little information found on the production of resonances (other than the T = 3/2, J = 3/2 isobar) at high energies (above 6 GeV). Here we present results on measurements of 4-prong events produced by 8 GeV/c positive pions in hydrogen where resonances are found to be frequently produced. The use of a higher incident energy was found to give a clearer separation of the resonances than is obtained at lower energies.

On 50,000 photographs taken in the Saclay 81cm hydrogen bubble chamber of 8 GeV/c positive pions from the CERN proton synchrotron, about 3,000 four-prong events were measured and analysed using the THRESH-GRIND-BAKE-SLICE-SUMX or similar system. To distinguish protons from pions, mean gap length measurements were made on tracks of up to 2 GeV/c momentum. For the reaction $\pi^+ p \rightarrow p\pi^+\pi^+\pi^-$ which allows a 4-constraint fit, all fits with probability greater than 1% were accepted, so that for this reaction protons of momentum greater than 2 GeV/c were identified by kinematic fitting. The laboratory momentum distribution of the protons and pions is shown in Figure 2, where it can be seen that there are very few protons of momentum greater than 2 GeV/c. It was accordingly assumed that for the other 4-prong interactions

---

+ On leave from Institute for Nuclear Research, Cracow
* On leave from the University of Bologna
** On leave from Institut für Theoretische Physik, Vienna

all tracks of greater than 2 GeV/c momentum were pions.

THE REACTION $\pi^+ p \rightarrow p\pi^+\pi^+\pi^-$

607 events of the reaction

$$\pi^+ p \rightarrow p\pi^+\pi^+\pi^- \qquad (1)$$

were found corresponding to a σ of 2.11 mb. In Figure 2 the $(p\pi^+)$ effective mass is plotted against the $(\pi^+\pi^-)$ effective mass. It can be seen that production of the N^{*++} $T = 3/2$, $J = 3/2$ isobar and the ρ-meson is very frequent, but as each event is plotted twice there is some background. If we require that one π^+ is in the N^{*++} isobar, then the plot, Figure 3, of the effective mass of the π^- with the other π^+, shows a strong peak at the ρ-meson mass and a peak at the f^o-meson mass. We can say that about half the events of reaction (1) are in reality one or other of the two-body reactions:

$$\pi^+ + p \rightarrow N^{*++} + \rho^o \qquad (2)$$

$$\pi^+ + p \rightarrow N^{*++} + f^o \qquad (3)$$

The apparent three-body reactions

$$\pi^+ + p \rightarrow N^{*++} + \pi^+ + \pi^- \text{ (NO } \rho^o\text{, NO } f^o \text{ production)} \qquad (4)$$

$$\pi^+ + p \rightarrow p + \pi^+ + \rho^o \text{ (NO } N^{*++} \text{ production)} \qquad (5)$$

also occur frequently as can be seen from Figure 2.

That the ρ^o-meson and the N^{*++} are produced peripherally can be seen in the Peyrou $(p_\perp - p_L^*)$ plots of Figure 4.

Considering reaction (5) only, the plot of the effective mass of $(\pi^+\rho)$ is shown in Figure 5, where the A_1 and A_2 mesons previously found[1),2)], can be seen. Where this figure differs from that of other groups using 3 to 4 GeV/c incident π^+, is that the background is very much lower here due probably to the higher energy of the incident pion allowing a better separation of the backward and forward-going resonances in the C.M. system. The central position of the A_1 and A_2 peaks reported by the German-British collaboration[1)], was 1.08 and 1.32 GeV. For the A_1 peak we find a value of 1.03 ± 0.02 GeV which may be different due to the lower background. For the A_2 peak, the value of 1.28 ± 0.02 is consistent with the earlier value.

Thus the reaction (5) which apparently gives a three-body final state in fact is mainly the two-body reactions $\pi^+ p \rightarrow p A_1$ and $\pi^+ p \rightarrow p A_2$.

THE REACTION $\pi^+ p \rightarrow p\pi^+\pi^+\pi^-\pi^o$

599 events of this reaction were observed corresponding to a cross-section of 2.1 ± 0.1 mb.

Here, some ρ^o and N^{*++} resonances are produced but in a smaller proportion than in reaction (1). The production of ω-mesons is shown by the distribution of the $(\pi^+\pi^-\pi^o)$ effective mass given in Figure 6. The experimental width of the ω-peak gives an indication of the resolution that can still be obtained at high energies by kinematical fitting of the entire event. It may also be noted on Figure 6 that the upper limit for η-meson production is appreciably smaller than for ω-production.

To search for the two- body reaction

$$\pi^+ + p \rightarrow \omega + N^{*++} \qquad (6)$$

the distribution of $(p\pi^+_a)$ effective mass was plotted for all events in which the $(\pi^+_b\pi^-\pi^o)$ effective mass was consistent with an ω-meson, where π^+_a and π^+_b are the two positive pions produced. This distribution, Figure 7, shows that reaction (6) does occur in at least one-third of all cases of ω-meson production.

The Cos θ^* distribution of ω-mesons, Figure 8, shows that they are produced in a peripheral manner in the forward C.M. direction.

OTHER 4-PRONG REACTIONS

The reactions

$$\pi^+ p \rightarrow \pi^+ + \pi^+ + \pi^+ + \pi^- + n \qquad (7)$$

$$\rightarrow \pi^+ + \pi^+ + \pi^+ + \pi^- + (n + q\pi^o) \text{ where } q \geq 1 \qquad (8)$$

$$\rightarrow p + \pi^+ + \pi^+ + \pi^- + (q\,\pi^o) \text{ where } q \geq 2 \qquad (9)$$

were found to have cross-sections of 0.86 ± 0.1, 2.5 ± 0.2 and 2.5 ± 0.2 mb, respectively. Evidence was found for the production of the $N^*_{3/2}$ isobar and of ρ-mesons, but less frequently than in reactions (1) and (5). The reactions are peripheral in character, but less so than in reaction (1).

CONCLUSIONS

1. Evidence has been obtained for abundant production of resonances in π-p interactions at energies as high as 8 GeV.

2. The resonances are mostly produced by peripheral interactions.

3. Because of the high incident momentum, the allocation of the secondary particles to forward and backward interaction vertices is facilitated, and hence the background is usually smaller than at lower energies.

4. The interactions leading to production of four charged secondaries, often proceed through initial formation of only two bodies ($N^{*} + \rho$, $N^{*} + f^{o}$, $N^{*} + \omega$, $p + A_1$, $p + A_2$), which subsequently decay.

ACKNOWLEDGMENTS

We are deeply indebted to the operating crews of the CERN proton synchrotron, the Saclay 81cm hydrogen bubble chamber and of the O2 beam. We would like to thank the computing staff at each laboratory.

REFERENCES

1) Aachen-Berlin-Birmingham-Bonn-Hamburg-London (I.C.)-München Collaboration, Phys. Letters, 10, 226 (1964).

2) G. Goldhaber, J.L. Brown, S. Goldhaber, J.A. Kadyk, B.C. Shen, G.H. Thrilling, Phys.Rev.Lett., 12, 336 (1964)

CAPTIONS FOR FIGURES

Figure 1 Laboratory momentum distribution of protons π^+ and π^- in reaction $\pi^+ p \to p\pi^+\pi^+\pi^-$.

Figure 2 Scatter diagram of $(p\pi^+_a)$ effective mass vs. $(\pi^+_b\pi^-)$ effective mass in reaction $\pi^+ p \to p\pi^+_a\pi^+_b\pi^-$.

Figure 3 $(\pi^+_a\pi^-)$ effective mass distribution in reaction $\pi^+ p \to p\pi^+_a\pi^+_b\pi^-$, when $\pi^+_b p)$ effective mass in N^{*++} region. The solid line is the phase space distribution, normalised to the total area .

Figure 4 Peyrou plots (transverse momentum vs. C.M. longitudinal momentum) of N^{*++} and of ρ^o in reaction $\pi^+ p \to p\pi^+\pi^+\pi^-$.

Figure 5 $(\rho^o\pi^+)$ effective mass distribution in reaction $\pi^+ p \to p\pi^+\pi^+\pi^-$, when neither $(\pi^+ p)$ combination is in the N^* region.

Figure 6 $(\pi^+\pi^-\pi^o)$ effective mass distribution in reaction $\pi^+ p \to p\pi^+\pi^+\pi^-\pi^o$. The solid line is the phase space distribution, normalised to the total area.

Figure 7 $(\pi^+_b p)$ effective mass distribution in reaction $\pi^- p \to p\pi^+\pi^+\pi^-\pi^o$, $(\pi^+_a\pi^-\pi^o)$ mass in ω region. The solid line is the phase distribution, normalised to the total area.

Figure 8 C.M. angular distribution of ω mesons produced in reaction $\pi^+ p \to p\pi^+\pi^+\pi^-\pi^o$.

$\pi^+ p \rightarrow p\pi^+\pi^+\pi^-$ at 8 GeV/c

FIG. 1

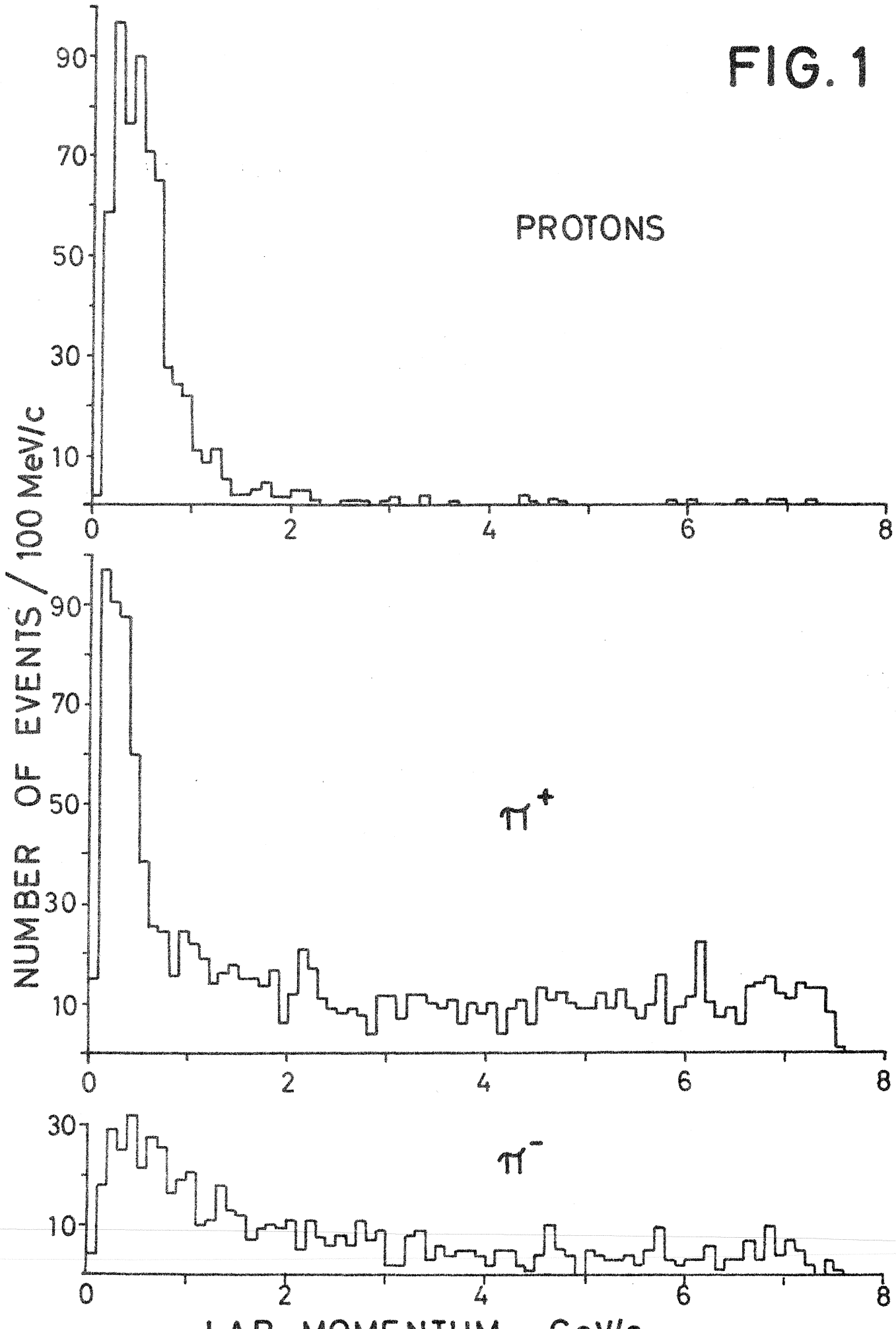

FIG. 2

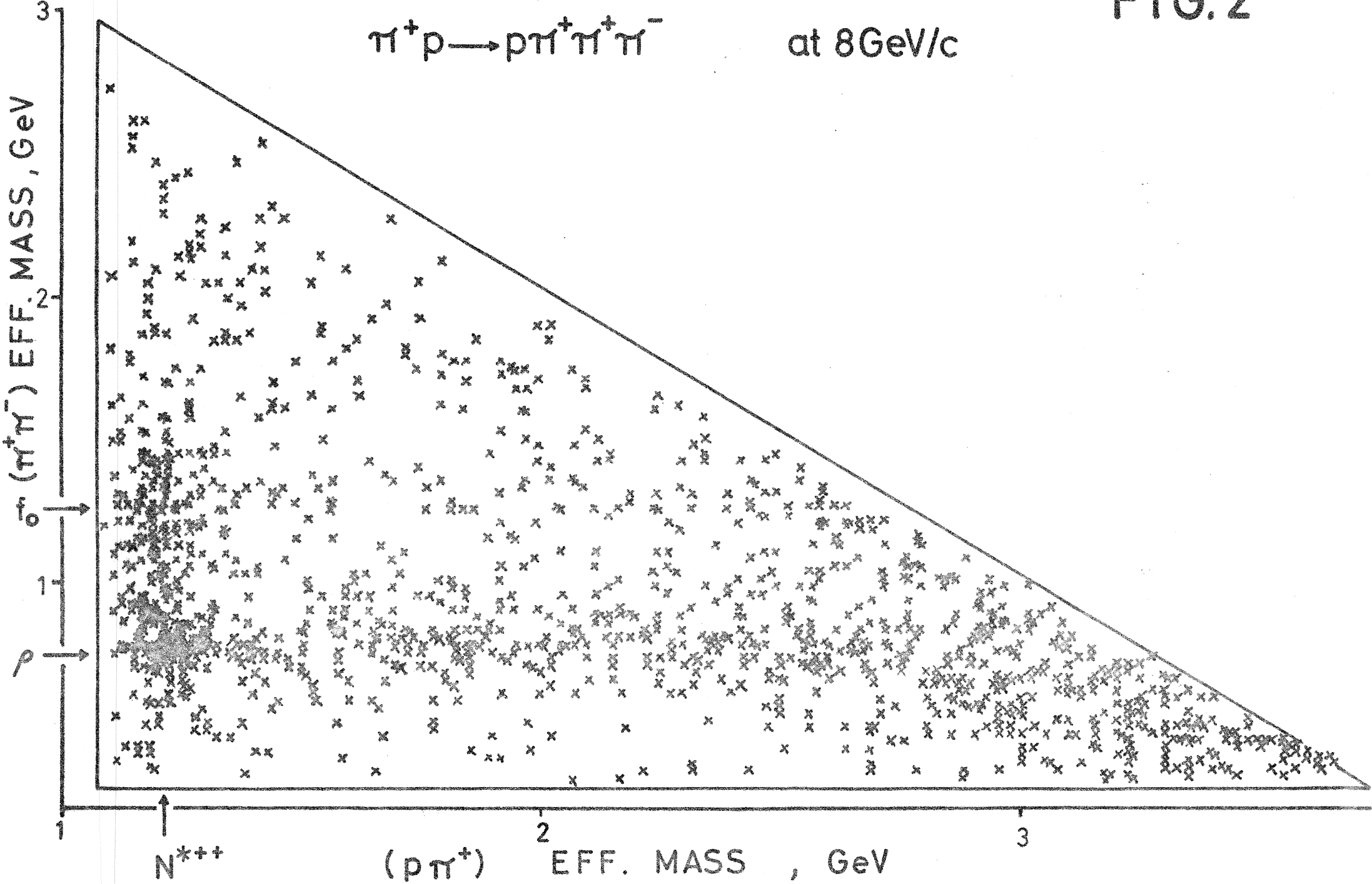
$\pi^+p \longrightarrow p\pi^+\pi^+\pi^-$ at 8GeV/c
$(\pi^+\pi^-)$ EFF. MASS, GeV
f_o
ρ
3
2
1
1
2
3
N^{*++}
$(p\pi^+)$ EFF. MASS, GeV

FIG. 3

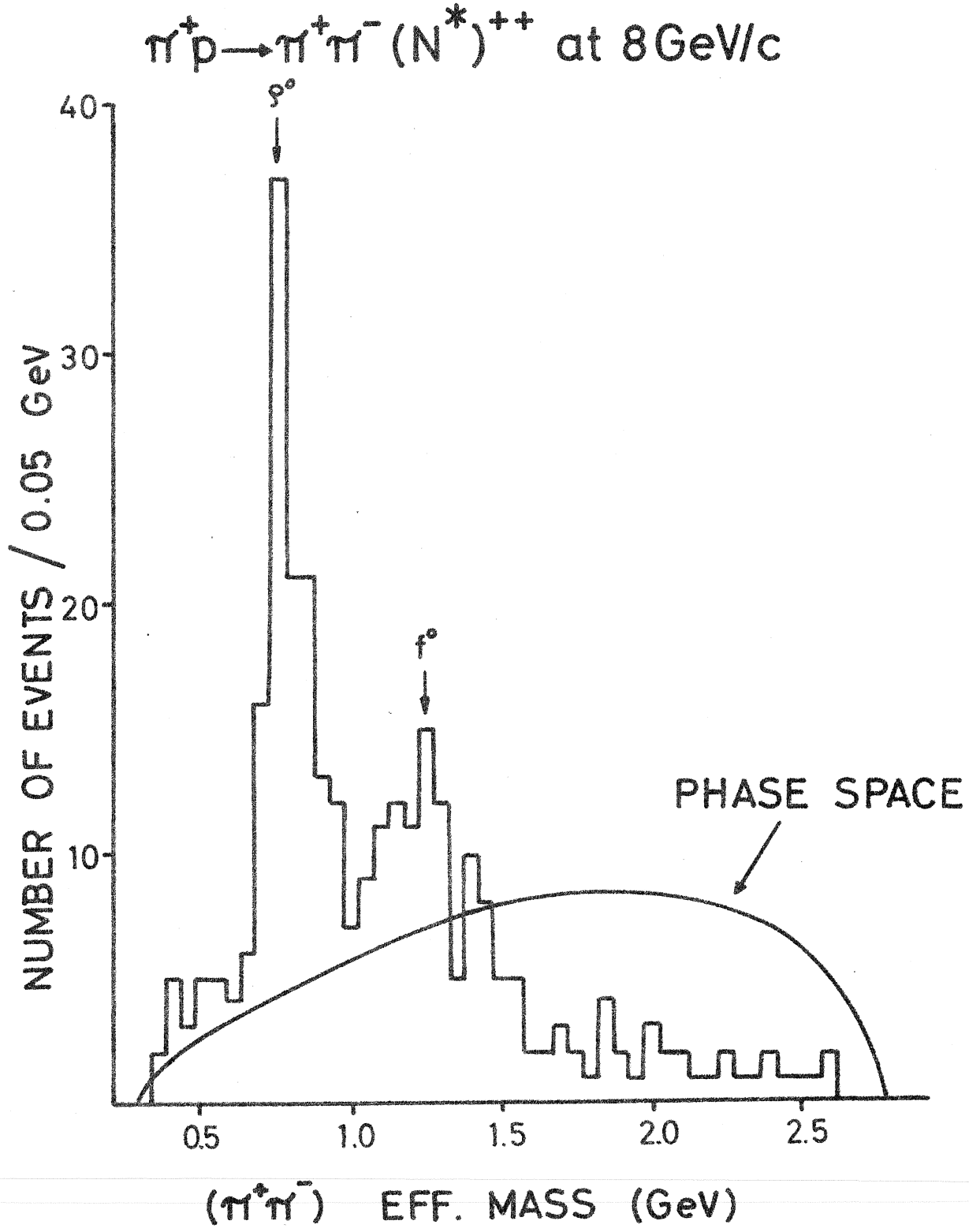
$\pi^+p \rightarrow \pi^+\pi^-(N^*)^{++}$ at 8 GeV/c
ρ^0
f^0
PHASE SPACE
NUMBER OF EVENTS / 0.05 GeV
40
30
20
10
0.5
1.0
1.5
2.0
2.5
$(\pi^+\pi^-)$ EFF. MASS (GeV)

FIG. 4

$\pi^+ p \rightarrow p\pi^+\pi^+\pi^-$ AT 8 GeV/c

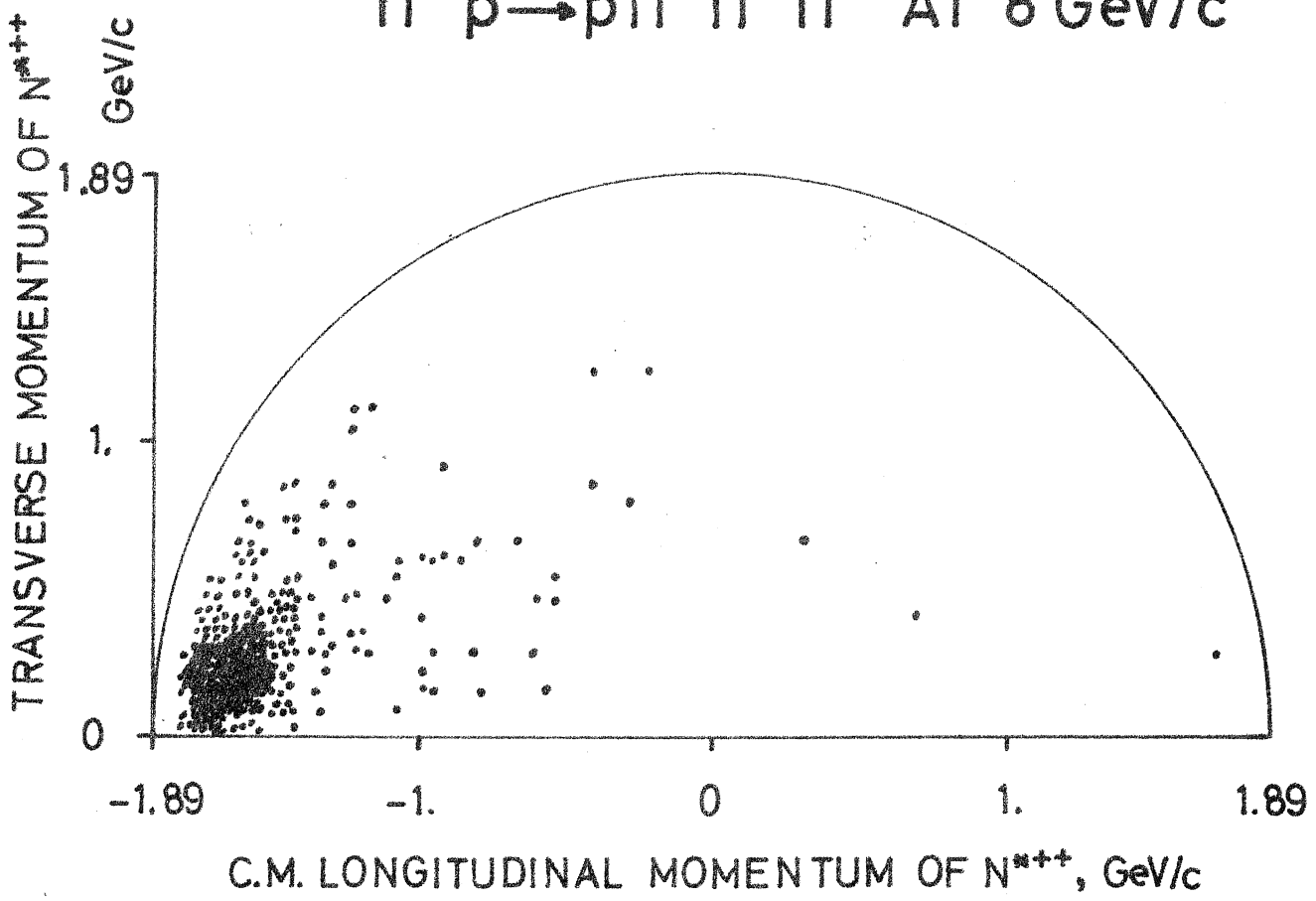

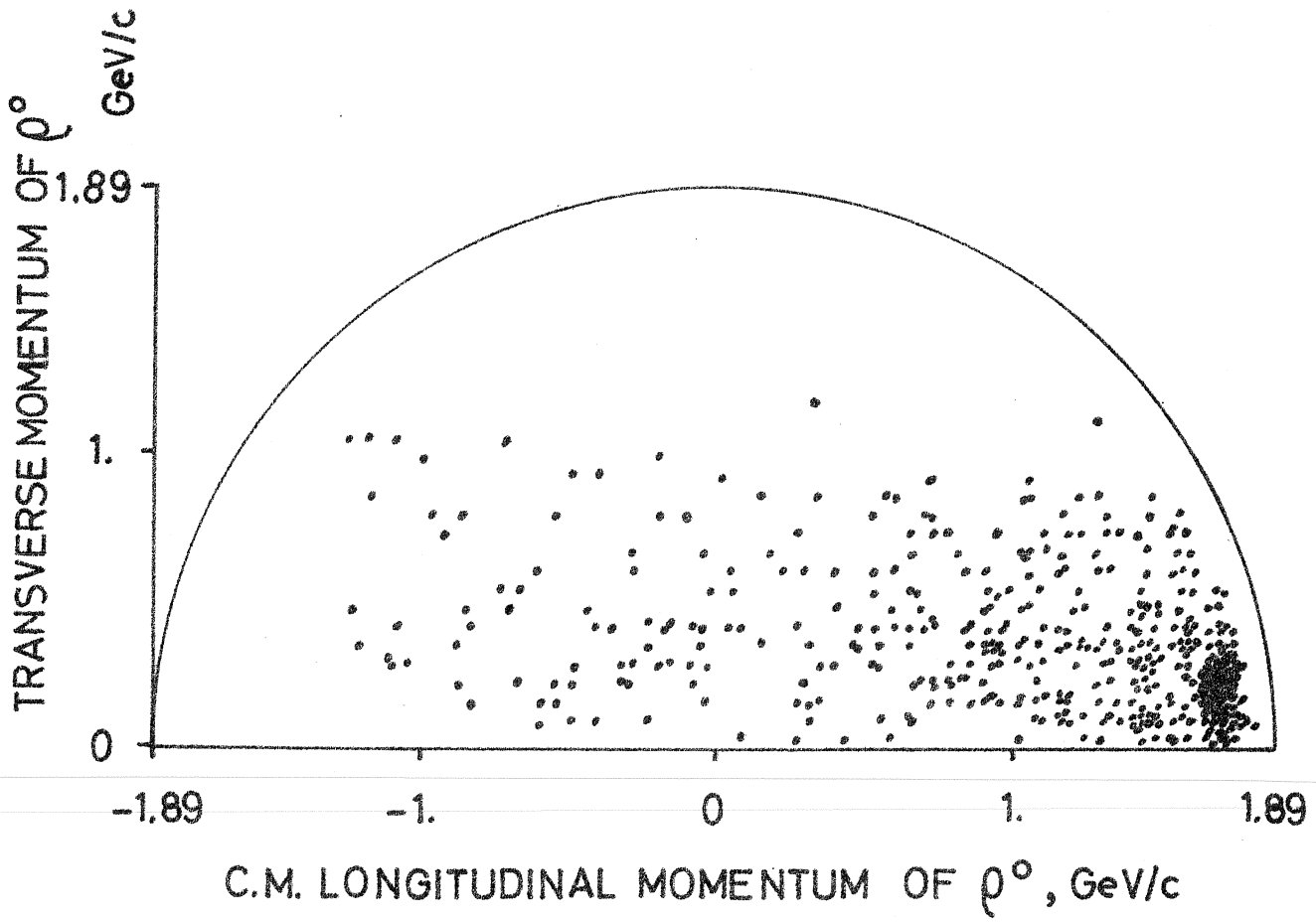

FIG. 5

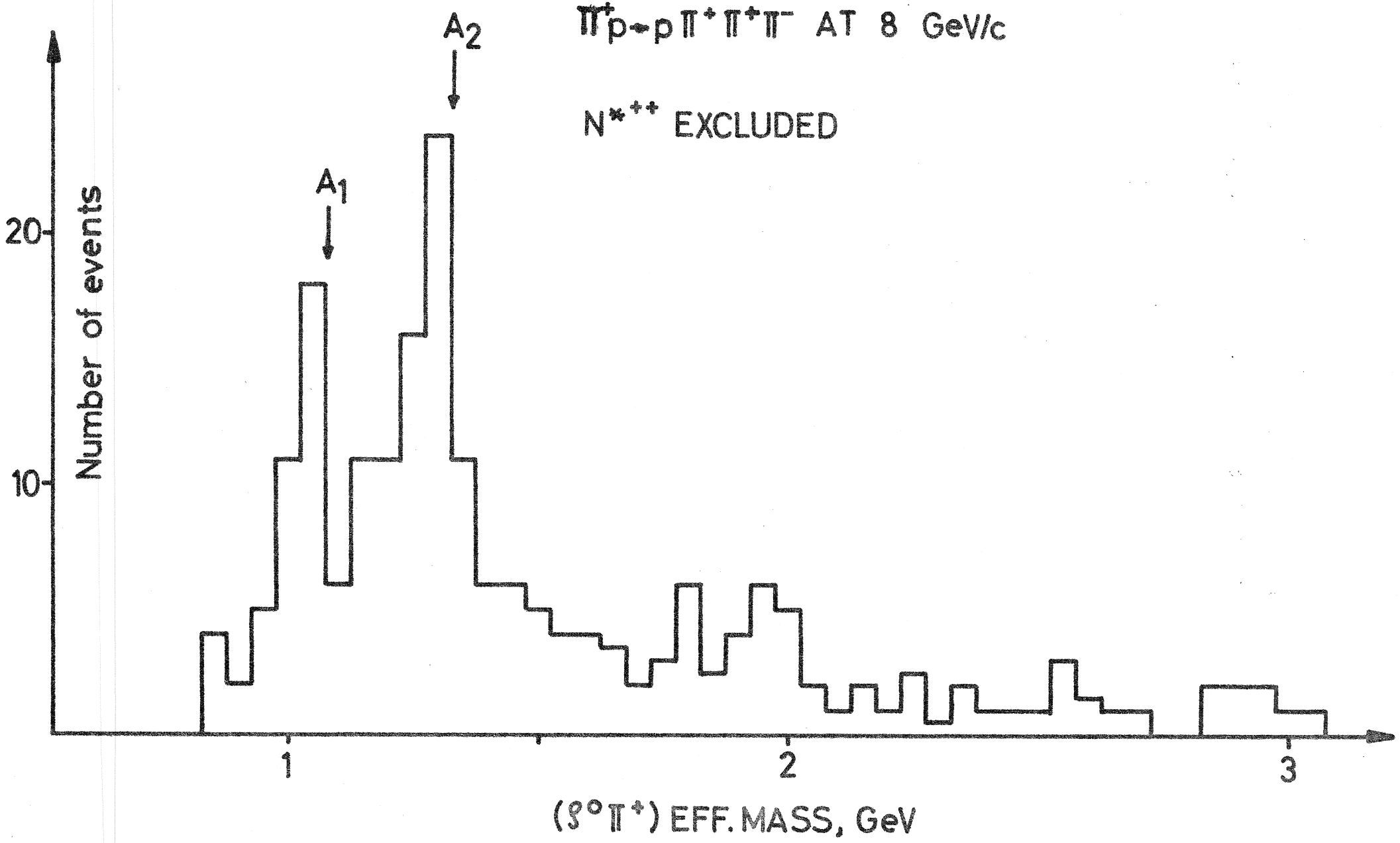
$\pi^+ p \to p\pi^+\pi^+\pi^-$ AT 8 GeV/c
N^{*++} EXCLUDED
A_1
A_2
Number of events
20
10
1
2
3
$(\beta^\circ\pi^+)$ EFF. MASS, GeV

FIG. 6

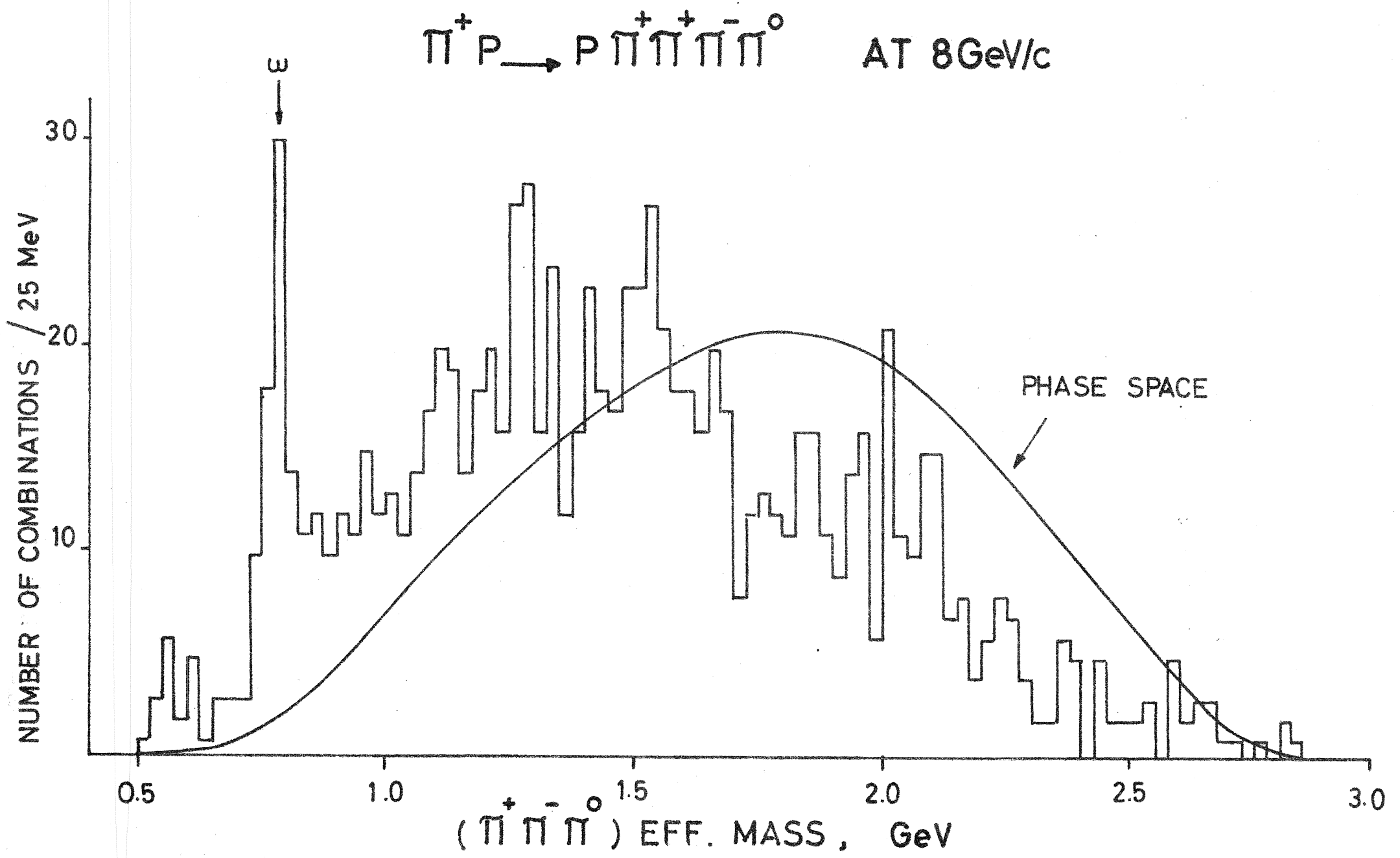
$\pi^+ P \longrightarrow P\,\pi^+\pi^+\pi^-\pi^\circ$ AT 8GeV/c
ω
PHASE SPACE
NUMBER OF COMBINATIONS / 25 MeV
30
20
10
0.5
1.0
1.5
2.0
2.5
3.0
$(\pi^+\pi^-\pi^\circ)$ EFF. MASS, GeV

FIG. 7

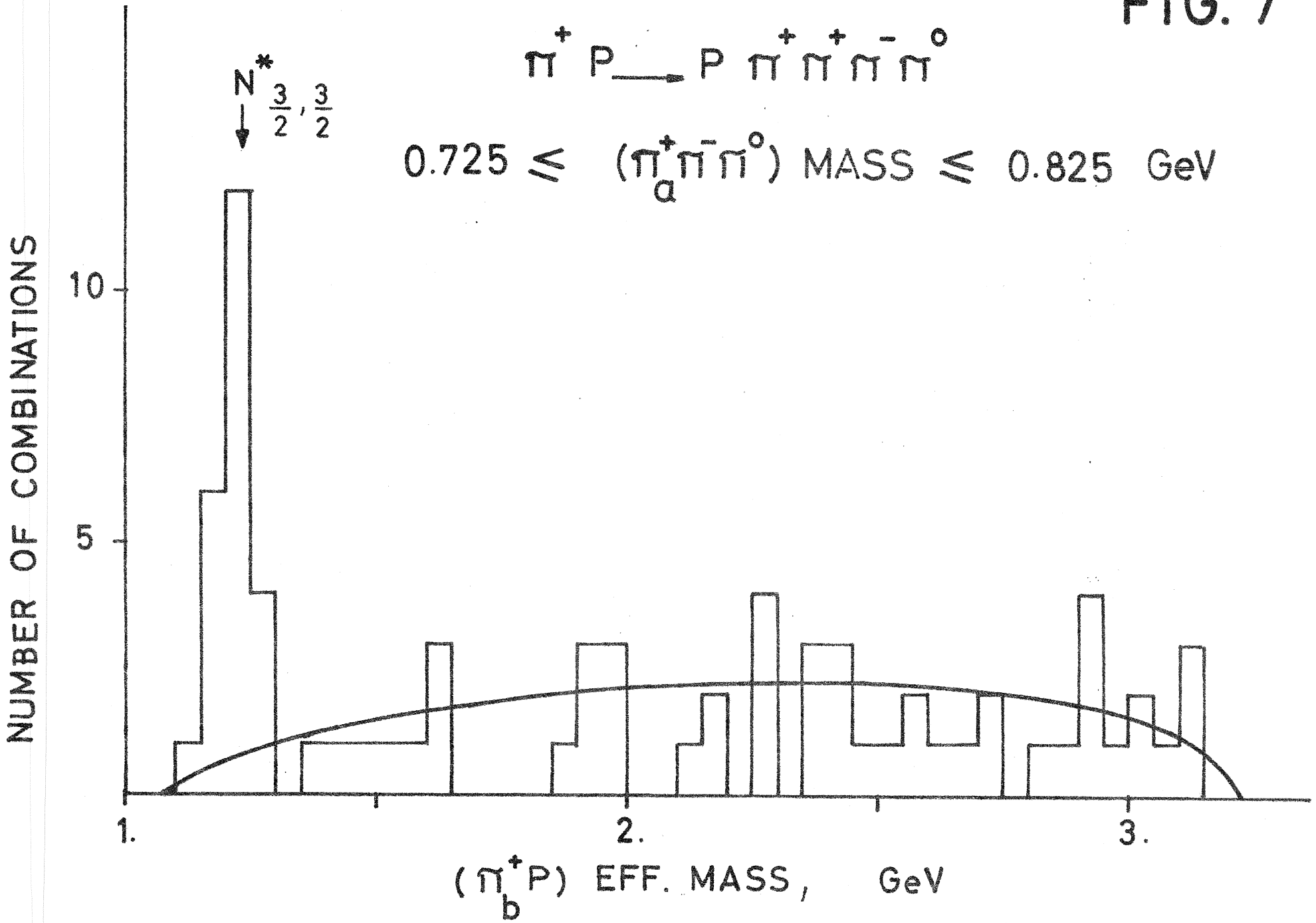
$\pi^+ P \longrightarrow P\,\pi^+\pi^+\pi^-\pi^\circ$
$0.725 \leq (\pi_a^+\pi^-\pi^\circ)$ MASS ≤ 0.825 GeV
$N^*_{\frac{3}{2},\frac{3}{2}}$
NUMBER OF COMBINATIONS
10
5
1.
2.
3.
$(\pi_b^+ P)$ EFF. MASS, GeV

FIG. 8

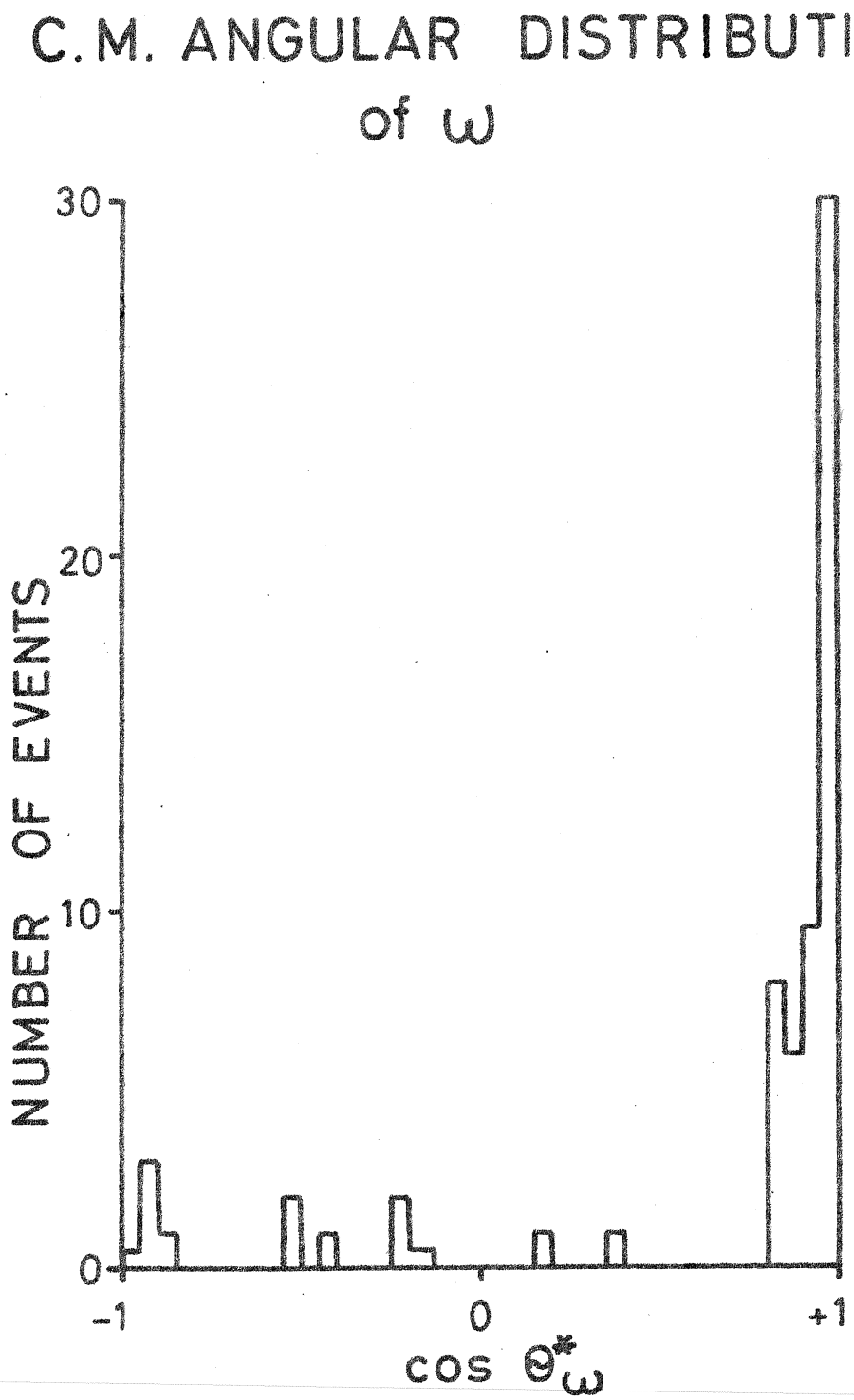
C.M. ANGULAR DISTRIBUTION
of ω
NUMBER OF EVENTS
30
20
10
0
-1
0
+1
cos θ*ω